Self-sorting microscale compartmentalized block copolypeptide hydrogels

Yintao Sun,[a] Laurent A. Bentolila[b,c] and Timothy J. Deming[a,b,c]*

[a] Department of Bioengineering, University of California, Los Angeles, CA 90095

[b] Department of Chemistry and Biochemistry, University of California, Los Angeles, CA 90095

[c] California NanoSystems Institute, University of California, Los Angeles, CA, 90095, USA

Abstract   Multicomponent interpenetrating network hydrogels possessing enhanced mechanical stiffness compared to their individual components were prepared via physical mixing of diblock copolypeptides that assemble by either hydrophobic association or polyion complexation in aqueous media. Optical microscopy analysis of fluorescent probe labeled multicomponent hydrogels revealed that the diblock copolypeptide components rapidly and spontaneously self-sort to form distinct hydrogel networks that interpenetrate at micron length scales. These materials represent a class of microscale compartmentalized hydrogels composed of degradable, cell-compatible components, which possess rapid self-healing properties and independently tunable domains for downstream applications in biology and additive manufacturing.

Hydrogels can display a broad range of structural and functional properties, and are being developed for many applications including as cell scaffolds, depots for therapeutic delivery, contact lenses, and coatings.[1-3] For certain applications, it is desirable to introduce multiple network components into hydrogels to alter mechanical properties or to create distinct functional environments, as can be found in biological materials.[1-4] Examples include covalently crosslinked double network hydrogels possessing

remarkable increased strength and toughness compared to their individual single network components,[5,6] as well as multicomponent hydrogels containing orthogonally self-assembled physical networks that can respond differently to various external stimuli, similar to cytoskeletal components found within cells.[7-11] Most of these hydrogels consist of networks that interpenetrate at molecular length scales, and there has been considerable recent effort to develop multicomponent hydrogels capable of possessing microscale compartmentalization akin to that found in cells and biological scaffolds.[12-14] Here, we report that mixtures of diblock copolypeptides are able to rapidly self-sort during assembly to spontaneously give dual compartment (DC) physical hydrogels containing distinct networks that interpenetrate at micrometer length scales. These DC hydrogels also possess significantly increased, and tunable, mechanical properties compared to their individual components (Figure 1).
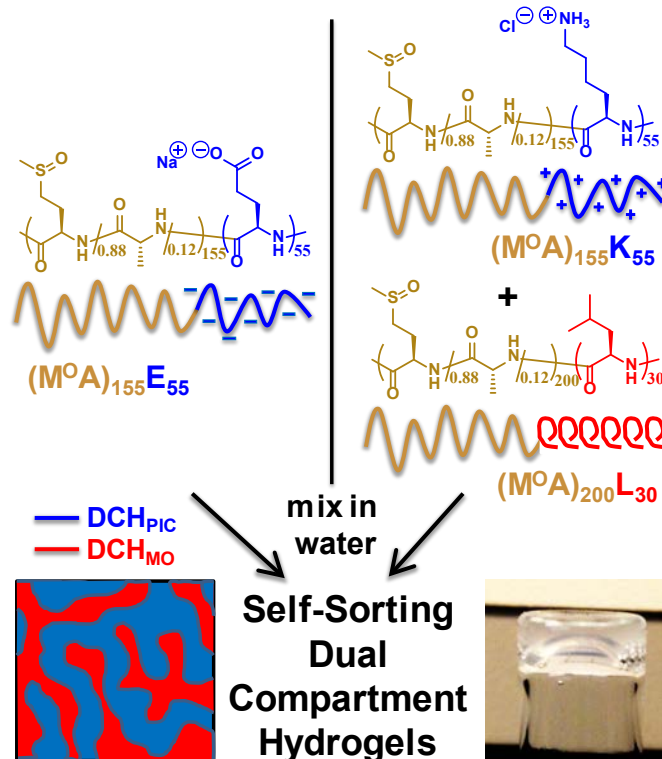

Figure 1. Schematic showing preparation of dual compartment diblock copolypeptide hydrogels (DCH$_{DC}$) via combination of (M^{O}A)$_{155}$E$_{55}$ + (M^{O}A)$_{155}$K$_{55}$ (DCH$_{PIC}$) and (M^{O}A)$_{200}$L$_{30}$ (DCH$_{MO}$), which

spontaneously self-sort into physical interpenetrating microscale networks in water via polyion complex and hydrophobic interactions, respectively.

Our lab has created a variety of diblock copolypeptide hydrogels (DCH),[15-18] where some have been developed for applications including localized delivery of molecules and cells within central nervous system tissues,[19,20] and as antimicrobial coatings for wounds and surgery.[21] DCH are readily formulated by addition of solid copolypeptide to aqueous media that may contain various molecules or cells, resulting in hydrogel formation at moderate temperatures and in different buffers or media.[15-18] These physically associated hydrogels are composed of branched and tangled nanoscale tape-like assemblies that can be deformed by applied stress and injected through narrow diameter needles, after which they rapidly self-heal into elastic gel networks.[15-18] DCH are also porous hydrogels that contain microscopic water-filled channels that allow for rapid diffusion of molecules within the networks.[15-18] Inspired by the multicomponent hydrogel strategies described above, we sought to introduce compartmentalization and mechanical enhancement into DCH through combination of different block copolypeptide components that would generate dual compartment DCH (hereafter DCH$_{DC}$). Since DCH networks are formed by direct self-assembly of copolypeptides in water, it was necessary to develop mixtures of DCH that could self-sort into two distinct networks during assembly, as opposed to co-assembling into a single network of mixed composition.

The challenge to prepare DCH$_{DC}$ is similar to that found in the self-assembly of mixtures of low molecular weight gelators (LMWG) used to form one-dimensional fibrils in water.[7-11] These LMWGs can also either co-assemble to give single networks, or self-sort to give DC hydrogels. Adams, van Esch, Smith, and others have reported strategies, relying on features including LMWG size and shape, and conditions such as pH, which allow LWMGs to self-sort into fibrils to form interpenetrating dual network hydrogels.[7-11] In these systems, the networks all interpenetrate at molecular length scales, and thus are homogeneous at larger scales.[7-11] Using external inputs such as photo-patterning or formation of aqueous

two-phase emulsions, microscale compartmentalization has also been introduced to some of these systems.[12,13] A significant recent achievement has shown that a mixture of LMWGs was capable of unprecedented spontaneous self-sorting at both the nanoscale and microscale, giving hierarchically compartmentalized hydrogels.[14] Some potential limitations of this system were the restricted compositions of components, weak mechanical properties (G′ ~ 40 Pa), and time required for full structure development (*ca.* 5 hours).[14] Inspired by these precedents, our design of DCH$_{DC}$ was focused on combination of block copolypeptides that assemble in water via orthogonal mechanisms in order to favor DC formation instead of co-assembly.

Most DCH are based on amphiphilic diblock copolypeptides that utilize assembly of hydrophobic segments in water to form hydrogels.[15,16] An example is DCH$_{MO}$, which is based upon nonionic, hydrophilic L-methionine sulfoxide (MO) and hydrophobic L-leucine residues.[18] We recently reported an alternative strategy for DCH formation where dual hydrophilic block copolypeptides assemble via polyion complexation between oppositely charged segments, hereafter DCH$_{PIC}$.[17] DCH$_{PIC}$ possess many features that are similar to amphiphilic DCH, but have improved stability against dilution. Since charged polypeptide segments were not expected to interact with hydrophobic polypeptide segments, the combination of amphiphilic copolypeptides with charged copolypeptides was explored as a means to prepare self-sorting DCH$_{DC}$ via self-assembly. The samples selected for this study were the previously reported poly(L-methionine sulfoxide-*stat*-L-alanine)$_{155}$-*block*-poly(L-lysine-HCl)$_{55}$, (M^{O}A)$_{155}$K$_{55}$, and poly(L-methionine sulfoxide-*stat*-L-alanine)$_{155}$-*block*-poly(L-glutamate-Na)$_{55}$, (M^{O}A)$_{155}$E$_{55}$ for DCH$_{PIC}$,[17] and poly(L-methionine sulfoxide-*stat*-L-alanine)$_{200}$-*block*-poly(L-leucine)$_{30}$, (M^{O}A)$_{200}$L$_{30}$ for amphiphilic DCH$_{MO}$ (Figure 1).[18] Non-ionic hydrophilic segments are essential for DCH$_{PIC}$ formation, and the readily prepared and degradable M^{O}A segments were chosen since they have been previously shown to give DCH that resist cell attachment and are cell compatible.[18] The different modes of assembly

in DCH$_{PIC}$ and DCH$_{MO}$ were expected to favor self-sorting during network formation to yield interpenetrating hydrogel networks.

The copolypeptides in Figure 1 were prepared as previously described by the stepwise addition of appropriate NCA monomers to growing chains initiated using Co(PMe$_3$)$_4$,[17,18] and gave samples with segment lengths and compositions that agreed with predicted values (see supporting information (SI), Table S1). Subsequent oxidation of methionine residues resulted in their conversion to methionine sulfoxides,[17,18] and removal of protecting groups in DCH$_{PIC}$ samples gave the final copolypeptides in high overall yields after purification (see Table S1). As control samples, single network hydrogels were prepared by either dissolving DCH$_{MO}$ copolypeptides or mixing aqueous solutions of DCH$_{PIC}$ copolypeptides at different concentrations in 1x PBS, which was chosen since this buffer provides improved DCH$_{PIC}$ formation compared to DI water.[17] As expected from prior studies, all samples formed translucent hydrogels over a range of copolypeptide concentrations as quantified using oscillatory rheology, and all were found to display elastic behavior (G′ » G″) over a range of frequency (see Figures S1, S2). All hydrogels were also found to break down under high strain, as expected for these physical hydrogels (see Figure S2).[17,18] Hydrogel stiffness (G′) was found to increase with sample concentration for all samples, and the specific compositions of DCH$_{MO}$ and DCH$_{PIC}$ were chosen to give comparable hydrogel stiffness at equivalent concentrations (see Figures S1, S2).

Next, we sought to prepare multicomponent hydrogels by combining DCH$_{MO}$ and DCH$_{PIC}$ copolypeptides during formulation. The successful formation of DC hydrogels may depend on the method of mixing, where there are many possible pathways. Since DCH$_{MO}$ forms networks directly upon dilution, while DCH$_{PIC}$ only forms networks upon mixture of both components, it was expected that relative rates of dissolution and mixing could affect resulting network structures. Since dissolution of (M^{O}A)$_{200}$L$_{30}$ is slow (minutes) compared to DCH$_{PIC}$ formation (seconds), we decided to fully dissolve (M^{O}A)$_{200}$L$_{30}$ before formation of the DCH$_{PIC}$ networks. Initially, dissolution of (M^{O}A)$_{155}$K$_{55}$ or (M^{O}A)$_{155}$E$_{55}$ copolypeptides

into separate viscous solutions/hydrogels of $(M^OA)_{200}L_{30}$ was compared against dissolution of $(M^OA)_{200}L_{30}$ copolypeptide into separate solutions of $(M^OA)_{155}K_{55}$ or $(M^OA)_{155}E_{55}$. It was observed that dissolution of $(M^OA)_{200}L_{30}$ into solutions of charged copolypeptides was more efficient than the reverse, likely since the viscosities of the charged copolypeptide solutions are much lower than that of dissolved $(M^OA)_{200}L_{30}$ thus allowing better physical mixing. Further, it was observed that $(M^OA)_{200}L_{30}$ dissolved much faster in $(M^OA)_{155}K_{55}$ solutions compared to $(M^OA)_{155}E_{55}$ solutions, possibly due to H-bonding interactions between M^O sulfoxide groups and the ammonium groups in $(M^OA)_{155}K_{55}$.[22]
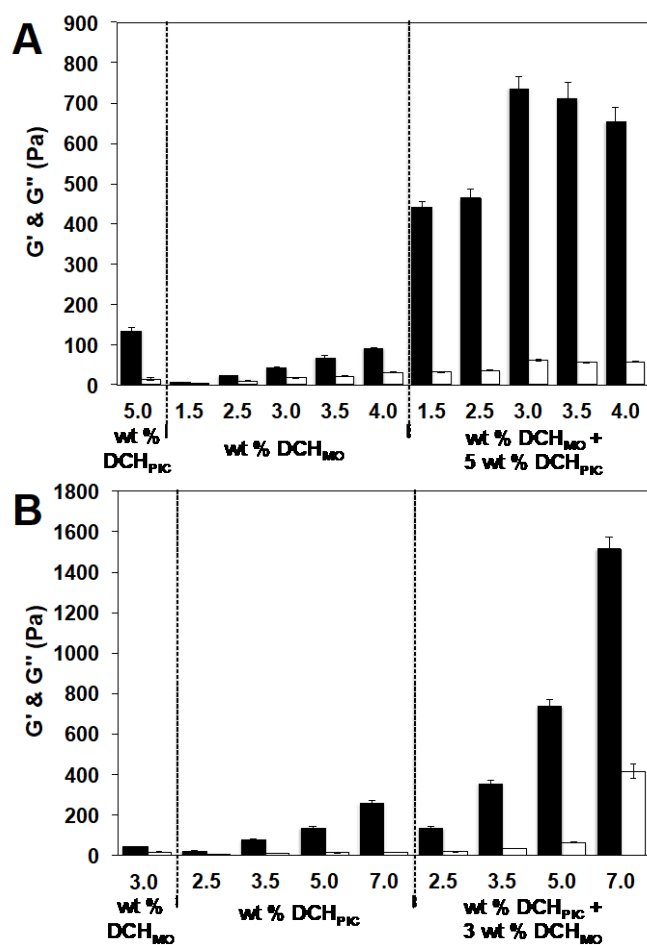

Figure 2. Mechanical properties of single and dual compartment diblock copolypeptide hydrogels. (A) G′ (Pa, black) and G″ (Pa, white) of DCH$_{DC}$ composed of 5 wt% DCH$_{PIC}$ and varying concentrations of DCH$_{MO}$ in 1× PBS buffer at 25 °C. Data for individual 5 wt% DCH$_{PIC}$ and DCH$_{MO}$ hydrogel components

6

at different concentrations in 1× PBS buffer at 25 °C are included for reference. (B) G′ (Pa, black), and loss modulus, G″ (Pa, white), of DCH$_{DC}$ composed of 3 wt% DCH$_{MO}$ and varying concentrations of DCH$_{PIC}$ in 1× PBS buffer at 25 °C. Data for individual 3 wt% DCH$_{MO}$ and DCH$_{PIC}$ hydrogel components at different concentrations in 1× PBS buffer at 25 °C are included for reference. All G′ and G″ values were measured at an angular frequency of 5 rad/s and a strain amplitude of 0.01, and are averages of triplicate runs with bars indicating standard deviations.

Studies on DCH$_{DC}$ formation were subsequently focused on the combination of solutions of (M^{O}A)$_{200}$L$_{30}$ dissolved in (M^{O}A)$_{155}$K$_{55}$ with solutions of (M^{O}A)$_{155}$E$_{55}$ (Figure 1). In the first series of experiments, the final concentration of DCH$_{PIC}$ was maintained at 5.0 wt% (combined mass of equimolar (M^{O}A)$_{155}$K$_{55}$ and (M^{O}A)$_{155}$E$_{55}$) while the final concentration of DCH$_{MO}$ was varied between 1.5 and 4.0 wt% (mass of (M^{O}A)$_{200}$L$_{30}$) (Figure 2A). To favor rapid dissolution, all the (M^{O}A)$_{200}$L$_{30}$ was dissolved in (M^{O}A)$_{155}$K$_{55}$ in 80% of the final volume 1x PBS, and this was then combined with the (M^{O}A)$_{155}$E$_{55}$ dissolved in 20% of the final volume 1x PBS. The resulting viscous solutions/hydrogels were then vortex mixed for 20 seconds and then let stand whereupon they all formed translucent hydrogels within 30 seconds. By visual inspection (i.e. tube inversion and agitation), all of the resulting DCH$_{DC}$ samples were more resistant to flow or deformation compared to their individual components. Rheological analysis of the samples verified that all the DCH$_{DC}$ samples were *ca.* 3 to 5 times stiffer (i.e. increased storage modulus G′) than the sum of their components (Figure 2A). All samples in Figure 2 were analyzed within one hour of preparation, and were found to show no differences in rheological properties over one week. It is worth noting that other methods of mixing, such as including (M^{O}A)$_{200}$L$_{30}$ in both precursor solutions and/or using equal volumes of precursor solutions, gave similar results, yet at the cost of slower initial (M^{O}A)$_{200}$L$_{30}$ dissolution.

The results in Figure 2A show that DCH$_{DC}$ stiffness increased with DCH$_{MO}$ concentration up to 3.0 wt%, but then reached a plateau and then began to decrease at higher concentrations. This plateau may

be due to incomplete physical mixing of DCH_{PIC} components since elasticity of the DCH_{MO} solutions increases significantly above 3.0 wt%. Holding the final DCH_{MO} concentration constant at 3.0 wt%, a second series of samples was prepared following the protocol described above where the final concentration of DCH_{PIC} was varied between 2.5 and 7.0 wt% (Figure 2B). All of these formulations formed translucent hydrogels within 30 seconds, and rheological analysis also showed that DCH_{DC} samples were significantly stiffer than the sum of their components (Figure 2B). The key difference here was the finding that there was no plateau in DCH_{DC} stiffness as DCH_{PIC} concentration increased, allowing flexibility in preparation of DCH_{DC} with a range of ratios of DCH_{PIC} to DCH_{MO}, where hydrogel stiffness increases with the amount of DCH_{PIC} added. These results showed that a consistent enhancement of hydrogel stiffness was present in all DCH_{DC} formulations.
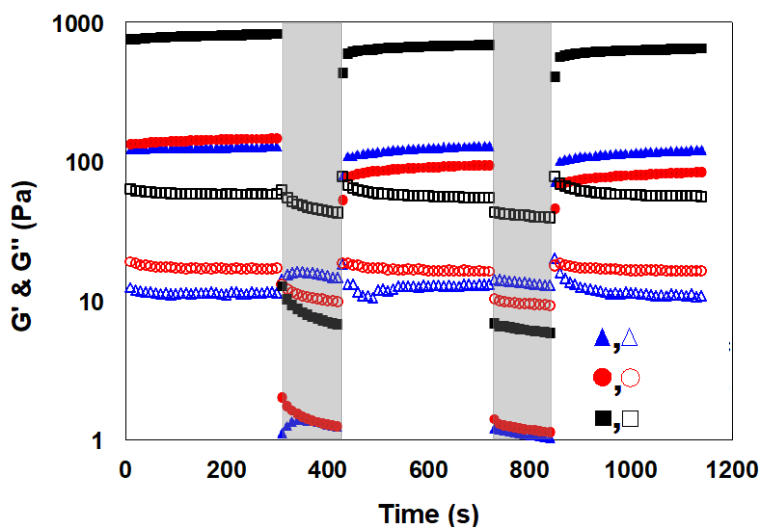

Figure 3. Mechanical recovery of 5 wt% DCH_{PIC}, 5 wt% DCH_{MO} and DCH_{DC} (3 wt% DCH_{MO} + 5 wt% DCH_{PIC}) over time in 1× PBS buffer at 25 °C (G′ = solid symbols; G″ = open symbols) after application of stepwise large-amplitude oscillatory break down (gray regions = strain amplitude of 10 at 10 rad/s for 120 s) followed by low-amplitude linear recovery (white regions = strain amplitude of 0.01 at 5 rad/s for 300 s).

A common characteristic of DCH_{MO} and DCH_{PIC} is that each possess thixotropic properties, or the ability to rapidly self-heal after deformation.[17,18,23] To determine if DCH_{DC} also possess self-healing mechanical properties, a sample of DCH_{DC} (3 wt% DCH_{MO} + 5 wt% DCH_{PIC}) was subjected to high amplitude oscillatory strain (1000 %), followed immediately by monitoring the recovery of elasticity over time by measuring G' at a much smaller strain (1%), Figure 3. During the initial 100 s of high strain amplitude, G' dropped significantly to below the level of G", indicating that the hydrogel was broken down to a viscous liquid. Upon switching to low strain amplitude, the sample began recovering its elastic properties over time with greater than 90% recovery of G' within seconds. It is possible some initial network structure is destroyed when the as-formed DCH_{DC} are subjected to high strain, yet this appears to be only a minor component, and most of the hydrogel stiffness is recovered after multiple strain breakdowns. Although DCH_{MO} and DCH_{PIC} are each known to self-heal individually (Figure 3), it was interesting to see that DCH_{DC} were also able to reform after exposure to repeated high strain. Near complete recovery of mechanical properties after repeated breakdown under high strain suggests that the self-assembled structure of DCH_{DC} is able to spontaneously reform and is not significantly altered after repeated stress. Furthermore, DCH_{DC} were also found to be resistant to dissolution in media similar to DCH_{PIC} formulations (see Figures S3, S4).[17] This media stability and rapid self-healing behavior are desirable as they allow deposition of hydrogel via injection through small bore needles, which has utility in applications for hydrogel depot formation *in vivo* as well as for additive manufacturing.

To better understand DCH_{DC} formation and the structural origins of DCH_{DC} mechanical behavior, individually fluorescent labeled DCH_{MO} and DCH_{PIC} components were prepared for analysis of DCH_{DC} using laser scanning confocal microscopy (LCSM). Previously, single component DCH were found to be composed of nanoscale networks that form hydrogels containing microscopic channels filled with water.[15,17] LCSM imaging of the DCH_{MO} component (red) in a dual labeled DCH_{DC} (3 wt% DCH_{MO} + 5

wt% DCH$_{PIC}$) sample, confirmed that microscale porosity of the DCH$_{MO}$ component was also present in DCH$_{DC}$ (Figure 4). Separate imaging of the DCH$_{PIC}$ component (green) revealed similar formation of a microporous DCH$_{PIC}$ network. Overlays of the green and red channels, in both 2D and 3D images, showed that the DCH$_{MO}$ and DCH$_{PIC}$ networks were mutually exclusive, forming segregated, interpenetrating DC structures of microscale dimensions (Figure 4). Images collected within one hour of sample preparation were indistinguishable from those collected after one week. These images support the formation of self-sorted compartmentalized networks in DCH$_{DC}$, where interpenetration does not occur at the level of individual fibrils or polymer chains as in other multicomponent hydrogels,[7-11] but at the much larger length scale of distinct microscopic hydrogel domains. The observed rapid formation of fully segregated dual networks in DCH$_{DC}$ may be due to limited or poor thermodynamic mixing of the different polypeptide components in aqueous media. The high molecular mass of the polypeptides, compared to LMWGs, may favor phase separation of the aqueous polypeptide solutions,[24] leading to the rapid segregation of DCH$_{PIC}$ and DCH$_{MO}$ components during assembly. The microscale DC morphology seen here also resulted in significant mechanical enhancement of DCH$_{DC}$ compared to its individual components. It is plausible that replacement of the aqueous channels of a single DCH network with an additional DCH network, as found in DCH$_{DC}$, provides mechanical reinforcement for both networks, thus inhibiting deformation of each and leading to enhanced stiffness.

In summary, physical mixing of hydrophobically assembled DCH$_{MO}$ and polyion complex assembled DCH$_{PIC}$ components in aqueous media was found to result in formation of DC hydrogels, DCH$_{DC}$, which possess enhanced mechanical stiffness while retaining the self-healing properties of the individual components. LSCM analysis of dual labeled fluorescent DCH$_{DC}$ revealed that DCH$_{MO}$ and DCH$_{PIC}$ components rapidly self-sort during formulation to spontaneously form distinct hydrogel networks that interpenetrate at micron length scales. These materials represent a new class of multicompartment hydrogel composed of degradable, cell-compatible components, which possess rapid

self-healing properties and independently adjustable and functionalizable domains for downstream applications in biology and additive manufacturing.
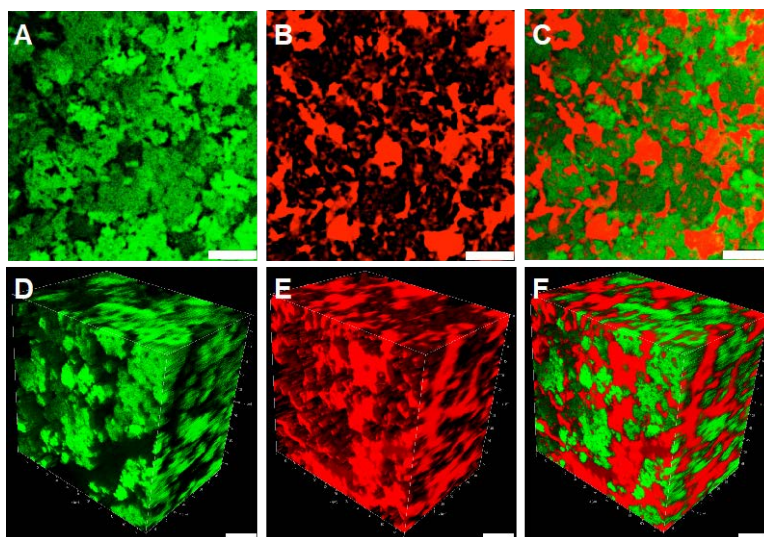

Figure 4. Laser scanning confocal microscopy (LCSM) images of DCH_{DC} (3 wt% DCH_{MO} + 5 wt% DCH_{PIC}). (A–C) LSCM images of DCH_{DC} prepared using Alexa Fluor 488 labeled $(M^OA)_{155}E_{55}$ and Alexa Fluor 633 labeled $(M^OA)_{200}L_{30}$ components that show separate interpenetrating networks of DCH_{MO} (red) and DCH_{PIC} (green) (z-thickness = 0.896 μm). (A) Alexa Fluor 488 channel, (B) Alexa Fluor 633 channel, (C) merged image of (A) and (B). (D-F) 3D renderings of DCH_{DC} z-slice stacks showing separate interpenetrating networks of DCH_{MO} (red) and DCH_{PIC} (green). (D) Alexa Fluor 488 channel, (E) Alexa Fluor 633 channel, (F) merged image of (D) and (E). All scale bars = 10 μm.

Supporting Information

The Supporting Information is available free of charge on the ACS Publications website at DOI: 10.1021/acsmacrolett.#######.

> Experimental procedures, spectral data, rheology data, hydrogel swelling data, and methods for all hydrogel characterization (PDF).

Author Information

Corresponding Author

* demingt@seas.ucla.edu

ORCID

Laurent A. Bentolila: 0000-0002-8758-1594

Timothy J. Deming: 0000-0002-0594-5025

Notes

The authors declare no competing financial interest.

References.

1) Peppas, N. A.; Huang, Y.; Torres-Lugo, M.; Ward, J. H.; Zhang, J. Physicochemical foundations and structural design of hydrogels in medicine and biology. *Annu. Rev. Biomed. Eng.* **2000**, *2*, 9–29.

2) Qiu, Y.; Park, K. Environment-sensitive hydrogels for drug delivery. *Adv. Drug Deliv. Rev.* **2012**, *64*, 49–60.

3) Murphy, W. L.; McDevitt, T. C.; Engler, A. J. Materials as stem cell regulators. *Nat. Mater.* **2014**, *13*, 547–557.

4) Haleem, A. M.; Chu, C. R. Advances in tissue engineering techniques for articular cartilage repair. *Oper. Technol. Orthop.* **2010**, *20*, 76– 89.

5) Gong, J. P.; Katsuyama, Y.; Kurokawa, T.; Osada, Y. Double-network hydrogels with extremely high mechanical strength. *Adv. Mater.* **2003**, *15*, 1155-1158.

6) Haque, M. A.; Kurokawa, T.; Gong, J. P. Super tough double network hydrogels and their application as biomaterials. *Polymer* **2012**, *53*, 1805-1822.

7) Heeres, A.; van der Pol, C.; Stuart, M.; Friggeri, A.; Feringa, B. L.; van Esch, J. Orthogonal self-assembly of low molecular weight hydrogelators and surfactants. *J. Amer. Chem. Soc.* **2003**, *125*, 14252–14253.

8) Moffat, J. R.; Smith, D. K. Controlled self-sorting in the assembly of 'multi-gelator' gels. *Chem. Commun.* **2009**, *0*, 316-318.

9) Morris, K. L.; Chen, L.; Raeburn, J.; Sellick, O. R.; Cotanda, P.; Paul, A.; Griffiths, P. C.; King, S. M.; O'Reilly, R. K.; Serpell, L. C.; Adams, D. J. Chemically programmed self-sorting of gelator networks. *Nat Commun.* **2013**, *4*, 1480.

10) Shigemitsu, H.; Fujisaku, T.; Tanaka, W.; Kubota, R.; Minami, S.; Urayama, K.; Hamachi, I. An adaptive supramolecular hydrogel comprising self-sorting double nanofibre networks. *Nat Nanotechnol.* **2018**, *13*, 165-172.

11) Viera, V. M. P.; Hay, L. L.; Smith, D. K. Multi-component hybrid hydrogels – understanding the extent of orthogonal assembly and its impact on controlled release. *Chem. Sci.* **2017**, *8*, 6981-6990.

12) Cornwell, D. J.; Daubney, O. J.; Smith D. K. Photopatterned multidomain gels: multi-component self-assembled hydrogels based on partially self-sorting 1,3:2,4-dibenzylidene-D-sorbitol derivatives. *J. Amer. Chem. Soc.* **2015**, *137*, 15486-15492.

13) Mytnyk, S.; Olive, A. G. L.; Versluis, F.; Poolman, J. M.; Mendes, E.; Eelkema, R.; van Esch, J. H. Compartmentalizing supramolecular hydrogels using aqueous multiphase systems. *Angew. Chem.* **2017**, *129*, 15119-15123.

14) Wang, Y.; Lovrak, M.; Liu, Q.; Maity, C.; le Sage, V. A. A.; Guo, X.; Eelkema, R.; van Esch, J. H. Hierarchically compartmentalized supramolecular gels through multilevel self-sorting. *J. Amer. Chem. Soc.* **2019**, *141*, 2847-2851.

15) Nowak, A. P.; Breedveld, V.; Pakstis, L.; Ozbas, B.; Pine, D. J.; Pochan, D.; Deming, T. J. Rapidly recovering hydrogel scaffolds from self-assembling diblock copolypeptide amphiphiles. *Nature* **2002**, *417*, 424-428.

16) Zhang, S.; Alvarez, D. J.; Sofroniew, M. V.; Deming, T. J. Design and synthesis of non-ionic copolypeptide hydrogels with reversible thermoresponsive and tunable physical properties. *Biomacromolecules* **2015**, *16*, 1331-1340.

17) Sun, Y.; Wollenberg, A. L.; O'Shea, T. M.; Cui, Y.; Zhou, Z. H.; Sofroniew, M. V.; Deming, T. J. Conformation directed formation of self-healing diblock copolypeptide hydrogels via polyion complexation. *J. Amer. Chem. Soc.* **2017**, *139*, 15114–15121.

18) Wollenberg, A. L.; O'Shea, T. M.; Kim, J. H.; Czechanski, A.; Reinholdt, L. G.; Sofroniew, M. V.; Deming, T. J. Injectable polypeptide hydrogels via methionine modification for neural stem cell delivery. *Biomaterials* **2018**, *178*, 527-545.

19) Zhang, S.; Burda, J. E.; Anderson, M. A.; Zhao, Z.; Ao, Y.; Cheng, Y.; Sun, Y.; Deming, T. J.; Sofroniew, M. V. Thermoresponsive copolypeptide hydrogel vehicles for CNS cell delivery. *ACS Biomater. Sci. Eng.* **2015**, *1*, 705-717.

20) Anderson, M. A.; O'Shea, T. M.; Burda, J. E.; Ao, Y.; Barlatey, S. L.; Bernstein, A. M.; Kim, J. H.; James, N. D.; Rogers, A.; Kato, B.; Wollenberg, A. L.; Kawaguchi, R.; Coppola, G.; Wang, C.; Deming, T. J.; He, Z.; Courtine, G.; Sofroniew, M. V. Required growth facilitators propel axon regeneration across complete spinal cord injury. *Nature* **2018**, *561*, 369-400.

21) Bevilacqua, M. P.; Huang, D. J.; Wall, B. D.; Lane, S. J.; Edwards III, C. K.; Hanson, J. A.; Benitez, D.; Solomkin, J. S.; Deming, T. J. Amino Acid Block Copolymers with Broad Antimicrobial Activity and Barrier Properties. *Macromolecular Biosci.* **2017**, *17*, 1600492.

22) Reyes, A.; Scott, R. M. Specific effects of dimethyl sulfoxide on the relative basicities of aliphatic amines. *J. Phys. Chem.* **1980**, *84*, 3600-3603.

23) Loebel, C.; Rodell, C. B.; Chen, M. H.; Burdick, J. A. Shear-thinning and self-healing hydrogels as injectable therapeutics and for 3D-printing. *Nat. Protoc.* **2017**, *12*, 1521-1541.

24) Mace, C. R.; Akbulut, O.; Kumar, A. A.; Shapiro, N. D.; Derda, R.; Patton, M. R.; Whitesides, G. M. Aqueous multiphase systems of polymers and surfactants provide self-assembling step-gradients in density. *J. Amer. Chem. Soc.* **2012**, *134*, 9094-9097.

TOC graphic

Rapid Self-Sorting Dual Compartment Hydrogels

$(M^OA)_{155}K_{55}$

$(M^OA)_{200}L_{30}$

$(M^OA)_{155}E_{55}$

mix in water

— DCH$_{PIC}$ — DCH$_{MO}$